Generation of isolated sub-10-attosecond pulses in spatially inhomogenous two-color fields

Xu Cao,[1] Shicheng Jiang,[1] Chao Yu,[1] Yunhui Wang,[1] Lihua Bai,[2,4] and Ruifeng Lu[1,3,*]

[1] *Department of Applied Physics, Nanjing University of Science and Technology, Nanjing 210094, China*
[2] *Department of Physics, Shanghai University, Shanghai 200444, China*
[3] *State Key Laboratory of Molecular Reaction Dynamics, Dalian Institute of Chemical Physics, Chinese Academy of Sciences, Dalian 116023, China*
[4] *lhbai@163.com*
[*] *rflu@njust.edu.cn*

Abstract: We present a theoretical investigation of high-order harmonic generation in spatially inhomogeneous two-color laser fields by solving three dimensional time dependent Schrödinger equation. The cutoff in the harmonic spectra can be significantly extended by means of our proposed method (i.e., from helium interacting with the plasmon-enhanced two-color laser fields), and an ultrabroad supercontinuum up to 1.5 keV is generated by selecting proper carrier-envelope phase of the controlling field. Moreover, classical trajectory extraction, time-dependent ionization and recombination rates, and time-frequency analyses are used to explain the generation of this ultrabroadband supercontinuum. As a result, an isolated 8.8 attosecond pulse can be generated directly by the superposition of the supercontinuum harmonics.

OCIS codes: (020.2649) Strong field laser physics; (190.7110) Ultrafast nonlinear optics; (340.7480) X-rays, soft x-rays, extreme ultraviolet (EUV).

References and links

1. C. Winterfeldt, C. Spielmann, and G. Gerber, "Colloquium: Optimal control of high-harmonic generation," Rev. Mod. Phys. **80**(1), 117–140 (2008).
2. P. M. Paul, E. S. Toma, P. Breger, G. Mullot, F. Auge, Ph. Balcou, H. G. Muller, and P. Agostini, "Observation of a train of attosecond pulses from high harmonic generation," Science **292**(5522), 1689–1692 (2001).
3. A. T. Le, R. R. Lucchese, M. T. Lee, and C. D. Lin, "Probing molecular frame photoionization via laser generated high-order harmonics from aligned molecules," Phys. Rev. Lett. **102**(20), 203001 (2009).
4. F. Krausz and M. Ivanov, "Attosecond physics," Rev. Mod. Phys. **81**(1), 163–234 (2009).
5. M. Hentschel, R. Kienberger, C. Spielmann, G. A. Reider, N. Milosevic, T. Brabec, P. Corkum, U. Heinzmann, M. Drescher, and F. Krausz, "Attosecond metrology," Nature **414**(6863), 509–513 (2001).
6. G. Sansone, E. Benedetti, F. Calegari, C. Vozzi, L. Avaldi, R. Flammini, L. Poletto, P. Villoresi, C. Altucci, R. Velotta, S. Stagira, S. De Silvestri, and M. Nisoli, "Isolated single-cycle attosecond pulses," Science **314**(5798), 443–446 (2006).
7. E. Goulielmakis, M. Schultze, M. Hofstetter, V. S. Yakovlev, J. Gagnon, M. Uiberacker, A. L. Aquila, E. M. Gullikson, D. T. Attwood, R. Kienberger, F. Krausz, and U. Kleineberg, "Single-cycle nonlinear optics," Science **320**(5883), 1614–1617 (2008).
8. K. J. Yuan and A. D. Bandrauk, "Single circularly polarized attosecond pulse generation by intense few cycle elliptically polarized laser pulses and terahertz fields from molecular media," Phys. Rev. Lett. **110**(2), 023003 (2013).
9. P. B. Corkum, "Plasma perspective on strong field multiphoton ionization," Phys. Rev. Lett. **71**(13), 1994–1997 (1993).
10. K. J. Schafer, B. R. Yang, L. F. DiMauro, and K. C. Kulander, "Above threshold ionization beyond the high harmonic cutoff," Phys. Rev. Lett. **70**(11), 1599–1602 (1993).
11. M. V. Frolov, N. L. Manakov, and A. F. Starace, "Wavelength scaling of high-harmonic yield: threshold phenomena and bound state symmetry dependence," Phys. Rev. Lett. **100**(17), 173001 (2008).
12. J. Tate, T. Auguste, H. G. Muller, P. Salières, P. Agostini, and L. F. DiMauro, "Scaling of wave-packet dynamics in an intense midinfrared field," Phys. Rev. Lett. **98**(1), 013901 (2007).
13. A. D. Shiner, C. Trallero-Herrero, N. Kajumba, H. C. Bandulet, D. Comtois, F. Légaré, M. Giguère, J. C. Kieffer, P. B. Corkum, and D. M. Villeneuve, "Wavelength scaling of high harmonic generation efficiency," Phys. Rev. Lett. **103**(7), 073902 (2009).

#220890 - $15.00 USD Received 12 Aug 2014; revised 23 Sep 2014; accepted 8 Oct 2014; published 16 Oct 2014

14. S. Kim, J. H. Jin, Y. J. Kim, I. Y. Park, Y. Kim, and S. W. Kim, "High-harmonic generation by resonant plasmon field enhancement," Nature **453**(7196), 757–760 (2008).
15. P. J. Schuck, D. P. Fromm, A. Sundaramurthy, G. S. Kino, and W. E. Moerner, "Improving the mismatch between light and nanoscale objects with gold bowtie nanoantennas," Phys. Rev. Lett. **94**(1), 017402 (2005).
16. M. Sivis, M. Duwe, B. Abel, and C. Ropers, "Nanostructure-enhanced atomic line emission," Nature **485**(7397), E1–E2, discussion E2–E3 (2012).
17. M. F. Ciappina, S. S. Aćimović, T. Shaaran, J. Biegert, R. Quidant, and M. Lewenstein, "Enhancement of high harmonic generation by confining electron motion in plasmonic nanostrutures," Opt. Express **20**(24), 26261–26274 (2012).
18. M. F. Ciappina, J. Biegert, R. Quidant, and M. Lewenstein, "High-order-harmonic generation from inhomogeneous fields," Phys. Rev. A **85**(3), 033828 (2012).
19. J. A. Pérez-Hernández, M. F. Ciappina, M. Lewenstein, L. Roso, and A. Zaïr, "Beyond carbon K-edge harmonic emission using a spatial and temporal synthesized laser field," Phys. Rev. Lett. **110**(5), 053001 (2013).
20. I. Yavuz, E. A. Bleda, Z. Altun, and T. Topcu, "Generation of a broadband xuv continuum in high-order-harmonic generation by spatially inhomogeneous fields," Phys. Rev. A **85**(1), 013416 (2012).
21. A. Husakou, S. J. Im, and J. Herrmann, "Theory of plasmon-enhanced high-order harmonic generation in the vicinity of metal nanostructures in noble gases," Phys. Rev. A **83**(4), 043839 (2011).
22. Z. Wang, P. Lan, J. Luo, L. He, Q. Zhang, and P. Lu, "Control of electron dynamics with a multicycle two-color spatially inhomogeneous field for efficient single-attosecond-pulse generation," Phys. Rev. A **88**(6), 063838 (2013).
23. M. Sivis, M. Duwe, B. Abel, and C. Ropers, "Extreme-ultraviolet light generation in plasmonic nanostructures," Nat. Phys. **9**(5), 304–309 (2013).
24. I. Y. Park, S. Kim, J. Choi, D. H. Lee, Y. J. Kim, M. F. Kling, M. I. Stockman, and S. W. Kim, "Plasmonic generation of ultrashort extreme-ultraviolet light pulses," Nat. Photonics **5**(11), 677–681 (2011).
25. M. Sivis and C. Ropers, "Generation and bistability of a waveguide nanoplasma observed by enhanced extreme-ultraviolet fluorescence," Phys. Rev. Lett. **111**(8), 085001 (2013).
26. Y. Y. Yang, A. Scrinzi, A. Husakou, Q. G. Li, S. L. Stebbings, F. Süßmann, H. J. Yu, S. Kim, E. Rühl, J. Herrmann, X. C. Lin, and M. F. Kling, "High-harmonic and single attosecond pulse generation using plasmonic field enhancement in ordered arrays of gold nanoparticles with chirped laser pulses," Opt. Express **21**(2), 2195–2205 (2013).
27. M. Krüger, M. Schenk, and P. Hommelhoff, "Attosecond control of electrons emitted from a nanoscale metal tip," Nature **475**(7354), 78–81 (2011).
28. G. Herink, D. R. Solli, M. Gulde, and C. Ropers, "Field-driven photoemission from nanostructures quenches the quiver motion," Nature **483**(7388), 190–193 (2012).
29. S. Watanabe, K. Kondo, Y. Nabekawa, A. Sagisaka, and Y. Kobayashi, "Two-color phase control in tunneling ionization and harmonic generation by a strong laser field and its third harmonic," Phys. Rev. Lett. **73**(20), 2692–2695 (1994).
30. T. Pfeifer, L. Gallmann, M. J. Abel, P. M. Nagel, D. M. Neumark, and S. R. Leone, "Heterodyne mixing of laser fields for temporal gating of high-order harmonic generation," Phys. Rev. Lett. **97**(16), 163901 (2006).
31. T. Pfeifer, L. Gallmann, M. J. Abel, D. M. Neumark, and S. R. Leone, "Single attosecond pulse generation in the multicycle-driver regime by adding a weak second-harmonic field," Opt. Lett. **31**(7), 975–977 (2006).
32. Y. H. Wang, H. P. Wu, Y. Qian, Q. Shi, C. Yu, Y. Chen, K. M. Deng, and R. F. Lu, "Laser-parameter effects on the generation of ultrabroad harmonic and ultrashort attosecond pulse in a long-plus-short scheme," J. Mod. Opt. **59**(19), 1640–1649 (2012).
33. Y. H. Wang, H. P. Wu, Y. Chen, Z. L. Lu, C. Yu, Q. Shi, K. M. Deng, and R. F. Lu, "Isolated sub-10 attosecond pulse generation by a 6-fs driving pulse and a 5-fs subharmonic controlling pulse," AIP Advances **2**(2), 022102 (2012).
34. C. L. Xia, X. L. Ge, X. Zhao, J. Guo, and X. S. Liu, "Isolated attosecond pulse generation from a model of Ar^+ cluster in a synthesized two-color laser pulse," Phys. Rev. A **85**(2), 025802 (2012).
35. C. L. Xia and X. S. Liu, "Quantum path control and isolated attosecond pulse generation with the combination of two circularly polarized laser pulses," Phys. Rev. A **87**(4), 043406 (2013).
36. H. C. Du, L. Y. Luo, X. S. Wang, and B. T. Hu, "Isolated attosecond pulse generation from pre-excited medium with a chirped and chirped-free two-color field," Opt. Express **20**(9), 9713–9725 (2012).
37. H. C. Du, L. Y. Luo, X. S. Wang, and B. T. Hu, "Attosecond ionization control for broadband supercontinuum generation using a weak 400-nm few-cycle controlling pulse," Opt. Express **20**(24), 27226–27241 (2012).
38. H. C. Du, Y. Z. Wen, X. S. Wang, and B. T. Hu, "Intense supercontinuum generation exceeding 300eV using a two-color field in combination with a 400-nm few-cycle control pulse," Opt. Express **21**(18), 21337–21348 (2013).
39. Z. N. Zeng, Y. Cheng, X. H. Song, R. X. Li, and Z. Z. Xu, "Generation of an extreme ultraviolet supercontinuum in a two-color laser field," Phys. Rev. Lett. **98**(20), 203901 (2007).
40. P. C. Li, C. Laughlin, and S. I. Chu, "Generation of isolated sub-20-attosecond pulses from He atoms by two-color midinfrared laser fields," Phys. Rev. A **89**(2), 023431 (2014).
41. R. F. Lu, P. Y. Zhang, and K. L. Han, "Attosecond-resolution quantum dynamics calculations for atoms and molecules in strong laser fields," Phys. Rev. E Stat. Nonlin. Soft Matter Phys. **77**(6), 066701 (2008).
42. R. F. Lu, H. X. He, Y. H. Guo, and K. L. Han, "Theoretical study of single attosecond pulse generation with a three-colour laser field," J. Phys. At. Mol. Opt. Phys. **42**(22), 225601 (2009).

#220890 - $15.00 USD Received 12 Aug 2014; revised 23 Sep 2014; accepted 8 Oct 2014; published 16 Oct 2014

43. H. X. He, R. F. Lu, P. Y. Zhang, Y. H. Guo, K. L. Han, and G. Z. He, "Theoretical investigation of the origin of the multipeak structure of kinetic-energy-release spectra from charge-resonance-enhanced ionization of H_2^+ in intense laser fields," Phys. Rev. A **84**(3), 033418 (2011).
44. H. X. He, R. F. Lu, P. Y. Zhang, K. L. Han, and G. Z. He, "Dissociation and ionization competing processes for H_2^+ in intense laser field: Which one is larger?" J. Chem. Phys. **136**(2), 024311 (2012).
45. H. X. He, R. F. Lu, P. Y. Zhang, K. L. Han, and G. Z. He, "Direct multi-photon ionizations of H_2^+ in intense laser fields," J. Phys. At. Mol. Opt. Phys. **45**(8), 085103 (2012).
46. J. Hu, K. L. Han, and G. Z. He, "Correlation quantum dynamics between an electron and D_2^+ molecule with attosecond resolution," Phys. Rev. Lett. **95**(12), 123001 (2005).
47. L. Q. Feng and T. S. Chu, "Generation of an isolated sub-40-as pulse using two-color laser pulses: Combined chirp effects," Phys. Rev. A **84**(5), 053853 (2011).
48. L. Q. Feng and T. S. Chu, "Nuclear signatures on the molecular harmonic emission and the attosecond pulse generation," J. Chem. Phys. **136**(5), 054102 (2012).
49. L. Q. Feng and T. S. Chu, "Role of excited states in asymmetric harmonic emission," Commun. Comput. Chem. **1**, 52–62 (2013).
50. X. Y. Miao and H. N. Du, "Theoretical study of high-order-harmonic generation from asymmetric diatomic molecules," Phys. Rev. A **87**(5), 053403 (2013).
51. X. Y. Miao and C. P. Zhang, "Multichannel recombination in high-order-harmonic generation from asymmetric molecular ions," Phys. Rev. A **89**(3), 033410 (2014).
52. C. Yu, H. X. He, Y. H. Wang, Q. Shi, Y. D. Zhang, and R. F. Lu, "Intense attosecond pulse generated from a molecular harmonic plateau of H_2^+ in mid-infrared laser fields," J. Phys. At. Mol. Opt. Phys. **47**(5), 055601 (2014).
53. A. D. Bandrauk and H. Z. Lu, "Enhanced ionization of the molecular ion H_2^+ in intense laser and static magnetic fields," Phys. Rev. A **62**(5), 053406 (2000).
54. M. Vafaee, H. Sabzyan, Z. Vafaee, and A. Katanforoush, "Detailed instantaneous ionization rate of H_2^+ in an intense laser field," Phys. Rev. A **74**(4), 043416 (2006).
55. X. M. Tong and Sh. I. Chu, "Probing the spectral and temporal structures of high-order harmonic generation in intense laser pulses," Phys. Rev. **61**(2), 021802 (2000).
56. X. Chu and Sh. I. Chu, "Optimization of high-order harmonic generation by genetic algorithm and wavelet time-frequency analysis of quantum dipole emission," Phys. Rev. **64**(2), 021403 (2001).
57. C. Jin, G. L. Wang, H. Wei, A. T. Le, and C. D. Lin, "Waveforms for optimal sub-keV high-order harmonics with synthesized two- or three-colour laser fields," Nat Commun **5**, 4003 (2014).

1. Introduction

Over the past decade, high-order harmonic generation (HHG) [1–3] has been popularly investigated since it is the most effective method to generate isolated attosecond pulses [4–8] which has been a subject of much interest in ultrafast science and technology. The HHG process for a single atom is well explained by the semiclassical three-step model [9,10]: First, the electron is ionized via tunneling toward the continuum, then it is accelerated by the laser field, finally, the electron recombines with the parent ion releasing the excess kinetic energy with a maximum cutoff given by $E_{\text{cutoff}} = I_p + 3.17U_p$. I_p is the ionization potential and $U_p = I/4\omega^2$ is the ponderomotive potential, where I and ω are intensity and frequency of the laser field, respectively. Because U_p is proportional to $I\lambda^2$, much effort has been done to extend the cutoff energy of HHG by increasing these two laser parameters. As is known to all, it is impossible to increase the intensity of the driving laser unlimitedly due to the limitation of the ionization potential and the ionization saturation of the atom. So increasing the wavelength of the driving laser looks a better way to achieve this goal. Unfortunately, numerical studies predict that harmonic efficiency falls dramatically when wavelength increases, with a very unfavourable $\lambda^{-(5\text{-}6)}$ scaling [11, 12] and even worse in experiments [13].

Recently, the experiment performed by Kim *et al.* [14] has shown that using the surface plasmon resonance spatially inhomogeneous laser field could be an efficient method for HHG. In this scheme, the weak input electric fields can be amplified more than 20 dB [14,15], which exceeds the threshold laser intensity for HHG in noble gases. However, Sivis *et al.* [16] claimed that they demonstrated extreme-ultraviolet emissions from gas-exposed nanostructures, and only observed line emission of neutral and ionized gas atoms, instead of HHG. These plasmon-enhanced fields can be understood by induced charges model. Furthermore, several theoretical schemes [17–22] have been suggested to use the plasmon-enhanced fields to extend the cutoff energy of HHG. Ciappina *et al.* [17,18] studied the enhancement of HHG in plasmonic nanostructures by confining electron motion, and

#220890 - $15.00 USD Received 12 Aug 2014; revised 23 Sep 2014; accepted 8 Oct 2014; published 16 Oct 2014

described the reasons for the cutoff extension. Coherent extreme ultraviolet photons beyond the carbon *K* edge has been proven from a temporally synthesized and spatially inhomogeneous strong laser field by Pérez-Hernández *et al.* [19]. Moreover, Yavuz *et al.* [20] obtained a 130 as pulse by employing a single four-optical-cycle plasmon-enhanced field.

So far, many different geometric shapes of the metal nanostructures have been designed to achieve plasmonic enhancement fields (e.g. inhomogeneous fields), such as plasmonic antennas [14,17,23], metallic waveguides [24,25], nanoparticles [26], and metal nanotips [27,28]. In general, different geometric shapes determine the form and the enhancement factor of the inhomogeneous field. From our numerical calculations, asymmetric inhomogeneous field is better for isolated attosecond pulse generation than symmetric inhomogeneous field. In particular, the spatially asymmetric distribution of the laser field will induce asymmetric recombination of electronic wave packets between the two sides of a target atom, which could reduce the interference in HHG emission for every optical cycle.

As for the generation of broad supercontinuum harmonic spectra, the two-colour field scheme [29–38] is an alternative method. For example, by taking this technique, Zeng *et al.* [39] demonstrated that an ultrabroad extreme ultraviolet supercontinuum spectrum can be obtained with a proper time delay between fundamental pulse and controlling pulse. Also, Li *et al* [40] claimed that the optimized two-color midinfrared laser pulse allows the HHG cutoff to be significantly extended and an isolated 18-attosecond pulse can be produced.

In the abovementioned theoretical works regarding the HHG in plasmonically enhanced fields by Lewenstein and associates [17–20] and by Yavuz *et al.* [20], only simple single laser or single-colour laser was used. In this paper, we theoretically consider the HHG in spatially inhomogeneous laser fields in combination with two-colour technique by solving three dimensional time dependent Schrödinger equation (3D TDSE). In our calculations, a 5 fs/800 nm fundamental laser and an 8 fs/1600 nm controlling laser are used and we found that the HHG cutoff can be strikingly extended, and an ultrabroadband supercontinuum is generated by selecting proper carrier-envelope phase (CEP) of the controlling field. Through classical trajectory extraction, time-dependent ionization and recombination rates as well as time-frequency analyses, we show that the ultrabroadband supercontinuum is generated by temporally controlling electronic recombination. The results indicate that an isolated 8.8-attosecond pulse which is much shorter than 1 atomic unit of time (24 as) can be gotten directly from our strategy.

The paper is organized as follows. We will briefly introduce the theoretical model and numerical method in section 2. The results and discussion are presented in section 3. The conclusion of our paper is in section 4.

2. Theoretical methods

In our quantum wave packet calculations, numerically solving 3D TDSE was conducted by our parallel computer code LZH-DICP [41] which was widely used to explore quantum dynamics processes of atoms and molecules in strong laser fields [42–52]. The laser electric field is linearly polarized along the z axis, and atomic units are used throughout this paper unless stated otherwise.

In the dipole approximation, the 3D TDSE is given in the cylindrical coordinates by [53,54]

$$i\frac{\partial\varphi(\rho,z;t)}{\partial t}=\left[T_\rho+T_z+V_C(\rho,z)+V_L(z,t)\right]\varphi(\rho,z;t), \tag{1}$$

where $T_\rho=-\frac{1}{2}\left(\frac{\partial^2}{\partial\rho^2}+\frac{1}{\rho}\frac{\partial}{\partial\rho}\right)$ and $T_z=-\frac{1}{2}\frac{\partial^2}{\partial z^2}$ denote the electronic kinetic energy operators. The conventional Coulomb potential $V_C(\rho,z)=-\alpha/\sqrt{\rho^2+z^2}$ is used with the

#220890 - $15.00 USD Received 12 Aug 2014; revised 23 Sep 2014; accepted 8 Oct 2014; published 16 Oct 2014

parameter α = 1.41 obtained by diagonalization of the potential matrix to match the ionization potential of 24.6 eV for the ground state of helium atom. $V_L(z,t)$ represents the coupling between the atom and the laser field. We define $V_L(z,t) = z(1+\beta|z|)E(t)$ as the spatially inhomogeneous coupling, where $E(t)$ is the temporal laser field and β determines the strength of the nonhomogeneity. In this work, we choose the parameter β = 0.0075. It is necessary to note that we employ a first order approximation to the spatially inhomogeneous fields, and we set spatial grid sizes as $-235 < z < 235$ a.u. which is equal to the experimental setup value of 20 nm after getting rid of the edge absorption length.

Then, by Fourier transforming the time-dependent dipole acceleration $a(t)$, the harmonic spectra are calculated by

$$P(\omega) = \left| \frac{1}{\sqrt{2\pi}} \int_0^T a(t) e^{-i\omega t} dt \right|^2, \tag{2}$$

To better investigate the temporal structures of HHG, we also perform time-frequency analyses by using the wavelet transformation of the dipole acceleration [55,56],

$$A(t,\omega) = \int a(t')\sqrt{\omega} W(\omega(t'-t)) dt', \tag{3}$$

where $W(\omega(t'-t))$ is the mother wavelet with the formula $W(x) = (\frac{1}{\sqrt{\tau}}) e^{ix} e^{-x^2/2\tau^2}$, and τ = 30 in our calculations. Finally, attosecond pulse can be obtained by superposing several harmonics in the plateau via

$$I(t) = \left| \sum_q \left(\int_0^t a(t') e^{-i\omega t'} dt' \right) e^{-iq\omega t} \right|^2, \tag{4}$$

where q is the harmonic order.

3. Results and discussions

The two-color laser field is synthesized by a 5 fs/800 nm fundamental field and an 8 fs/1600 nm controlling field as

$$E(t) = E_1 f_1(t-T_0)\cos(\omega_1(t-T_0)+\phi_1) + E_2 f_2(t-T_0)\cos(\omega_2(t-T_0)+\phi_2). \tag{5}$$

The laser peak intensities corresponding to E_1 and E_2 are $I_1 = 1.0 \times 10^{15}$ W/cm^2 and $I_2 = 2.0 \times 10^{14}$ W/cm^2, respectively. Actually, the quoted intensities are the plasmonic-enhanced values, not the input laser intensities and the latter could be several orders of magnitude smaller. We know that the general metal nanostructures cannot sustain intensities much above 10^{13} W/cm^2 [23], so this sets a requirement on the enhancement factors needed. Gaussian envelope $f(t-T_0)$ is used, and pulse duration of 5 fs (and 8 fs) is the FWHM of single laser. Here, T_0 = 11 fs, ω_1, ω_2 are the frequencies of the 800 nm and the 1600 nm pulses, respectively, and φ_1, φ_2 are the corresponding carrier-envelope phases (CEPs). In the two-color laser field, we use the frequency of the fundamental field to define the ponderomotive potential because of the relatively weak intensity of controlling field. In two-color inhomogeneous laser field, there are many parameters can be controlled, and we fixed fundamental phase $\varphi_1 = 0$. The temporal shape of the enhanced two-color laser field by plasmonic antennas with controlling phase $\varphi_2 = 0$ and $\varphi_2 = 1.56\pi$ are shown in Fig. 1(a). We can see that laser field is strongly changed by alter the phase φ_2, which could be used to control the dynamics of the electrons.

#220890 - $15.00 USD Received 12 Aug 2014; revised 23 Sep 2014; accepted 8 Oct 2014; published 16 Oct 2014

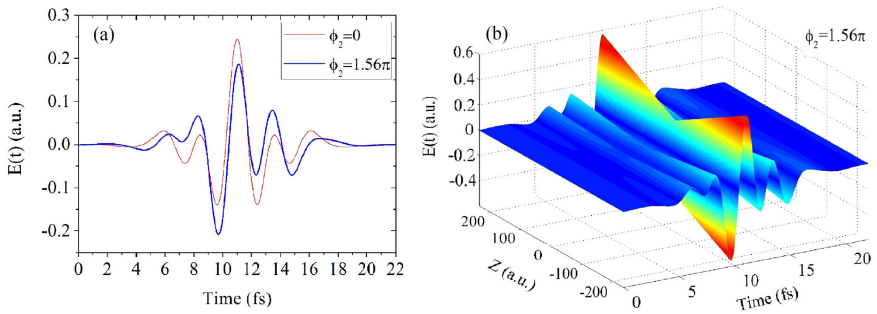

Fig. 1. (a) The temporal shape of the two-color laser field with controlling phase $\varphi_2 = 0$ (red line) and $\varphi_2 = 1.56\pi$ (blue line). (b) Coupling field in time and space for the $\varphi_2 = 1.56\pi$.

When in combination with the spatially inhomogeneous coupling, Fig. 1(b) shows coupling field in time and space for the $\varphi_2 = 1.56\pi$ case in our model. In Fig. 1(b), the field strength is amplified from the coordinates' origin to the simulation box's boundaries, and the field is symmetrical in space. Comparing with the homogeneous field, electrons can be tunneling ionized with the same intensity of the field at the coordinates' origin, but they will get higher energy in acceleration due to the higher field strength in other space. So, the plasmonic-enhanced spatially inhomogeneous laser field not only ensure that the field strength in the coordinates' origin is not above the ionization saturation for the gas but also extend the HHG cutoff by higher field strength in other spatial region.

Figure 2 provides the comparison among the HHG spectra generated by single-color homogeneous laser field (red line), two-color homogeneous laser field with $\varphi_2 = 0$ (green line) and two-color inhomogeneous laser field with $\varphi_2 = 0$ (orange line) and 1.56π (blue line). Here, the single-color field is identical to the fundamental field in the two-color case and the parameters of the two-color laser are the same as those in Fig. 1. Compared with the single-color homogeneous field, the position of the harmonic cutoff shifts from 217 eV to 580 eV in two-color homogeneous laser field. By combining with the spatially inhomogeneous scheme, the cutoff for the controlling laser with no phase delay can be extended to 910 eV, however, the plateau is not very smooth. There is no qualitatively monotonous relationship between the width of plateau and the CEP, which has been elucidated in our previous work [32], so we don't present all HHG spectra for different CEP. Most remarkably, with optimal controlling phase $\varphi_2 = 1.56\ \pi$, an ultrabroad supercontinuum spectrum in which the cutoff is amazedly extended to 2280 eV is generated.

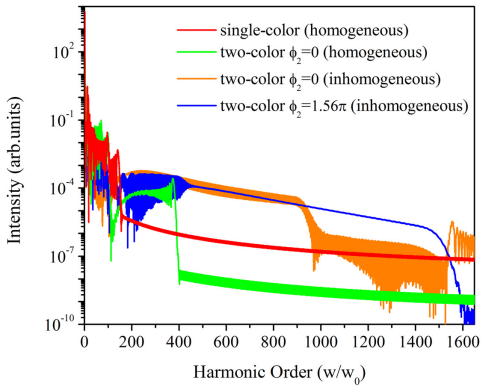

Fig. 2. HHG spectra generated by single-color homogeneous laser field (red line), two-color homogeneous laser field with $\varphi_2 = 0$ (green line) and two-color inhomogeneous laser field with $\varphi_2 = 0$ (orange line) and $\varphi_2 = 1.56\pi$(blue line).

#220890 - $15.00 USD Received 12 Aug 2014; revised 23 Sep 2014; accepted 8 Oct 2014; published 16 Oct 2014

To address the physics of this ultrabroadband supercontinuum spectrum, the time-frequency analysis of HHG is shown in Fig. 3. We clearly see that there are two recollision time points of electron, and only the early recollision at t = 11.5 fs contributes to the supercontinuum spectrum. Moreover, the maximum recollision energy is consistent with the cutoff energy of HHG spectrum. It also indicates that the broad supercontinuum results from only single short quantum path which is desired to generate shorter attosecond pulse [57].

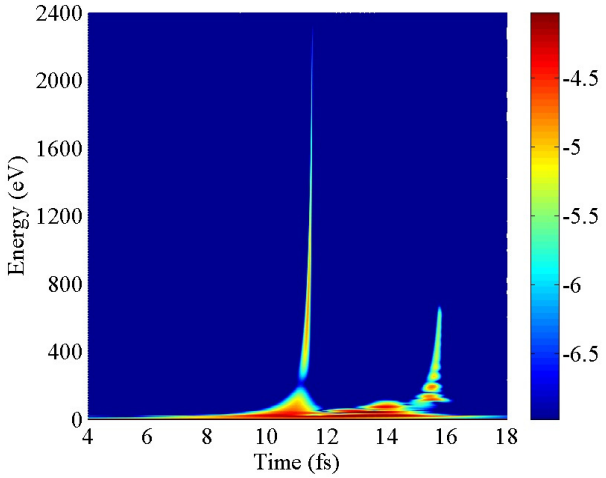

Fig. 3. The time-frequency analysis of HHG in Fig. 2 for the two-color inhomogeneous laser field with $\varphi_2 = 1.56\pi$. The color bar is on logarithmic scale and in arbitrary unit.

To further verify this ultrabroad supercontinuum spectrum from quantum calculations, the classical Newtonian equation

$$\ddot{z}(t) = -\nabla_z V_L(z,t), \tag{6}$$

for an electron moving in the aforementioned spatially inhomogeneous two-color laser field is solved, where $V_L(z,t)$ is the spatially inhomogeneous coupling in section 2. Thus, the final equation of electron motion is

$$\ddot{z}(t) = -(1+2\beta|z|)E(t). \tag{7}$$

Generally, the classical electron trajectory can be derived. The electrons are assumed starting with zero velocity and the position at every time points. The time step is set as 0.02 a.u. which is equal to the time step of 3D TDSE calculation. Then, the velocity and the position can be calculated by numerical integrating $\ddot{z}(t)$ under a laser condition as $\dot{z}(t) = \sum_{t_0}^{t} \ddot{z}(t)dt$ and $z(t) = \sum_{t_0}^{t} \dot{z}(t)dt$. At last, the recollision electrons can be selected when the positions of the electrons are back near the origin of coordinates. The ionization and recollision energies can be calculated using $E = \dot{z}^2/2$. Figure 4(a) shows the classical ionization and recollision energy plots in the spatially inhomogeneous two-color laser field and the laser parameters are identical to Fig. 3. Unusually, we can find three dominant recollision peaks which are labeled as P_1, P_2, P_3, but there are only two peaks as P_2, P_3 consistent with the two recollision time points in time-frequency analysis. It means the first recollision peak P_1 almost doesn't contributed to the ultrabroad supercontinuum spectrum. In more details, there are two recollision trajectories localized in P_3, and they interfere with each other resulting in the periodic structure around the time of 16 fs in Fig. 3. As is well known, the classical analysis

#220890 - $15.00 USD Received 12 Aug 2014; revised 23 Sep 2014; accepted 8 Oct 2014; published 16 Oct 2014

cannot provide the electron recombination probability which is one of the most important factors in the HHG according to three-step model.

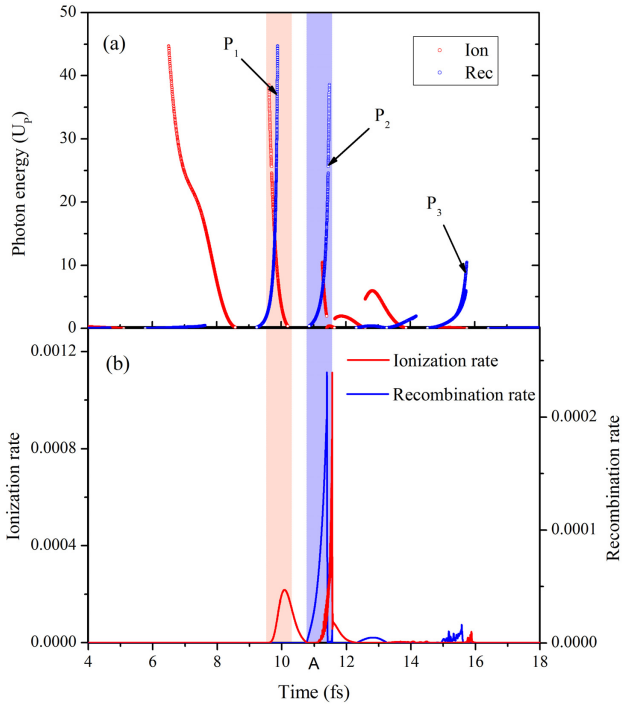

Fig. 4. (a) The time-dependent classical ionization and recollision energy analysis. P_1, P_2 and P_3 indicate the three dominant peaks of the recollision. (b) The time-dependent ionization rate and recombination rate in the spatially inhomogeneous two-color laser field. The laser parameters are identical to those in Fig. 3.

This can be understood from the time dependent ionization rate and recombination rate in Fig. 4(b), which are calculated by the flux operator method as

$$P(t) = \int_0^{\rho} \int_{-z}^{z} \mathrm{Im}[\varphi^* \delta(z - z_0) \frac{\partial}{\partial z} \varphi] dz \rho d\rho, \tag{8}$$

where z_0 are the position of flux analysis for ionization or recombination. The results show a dominant recombination at t = 11.5 fs, which is consistent with the recollision peak P_2 in Fig. 4(a) (see blue region). Although the first recollision peak P_1 in Fig. 4(a) has higher recollision energy, very small recombination rate at P_1 means it has no contribution in HHG. We of course calculate other controlling phase, and the electronic recombination can be temporally controlled by properly selecting the controlling phase, here only $\varphi_2 = 1.56\ \pi$ with maximum ultrabroad supercontinuum is discussed.

In Fig. 5(a), we show an isolated 8.8-as pulse which is much shorter than the atomic unit of time of 24 as is obtained by superposing the supercontinuum harmonics from the 1200th to the 1500th order without any phase compensation. It also illustrates that there is only one attosecond pulse emission in the whole time range, which will be a promising tool for attosecond resolution probe. For a closer connection to a possible experimental realization, a Gaussian band-pass function is used as a filter. Then, a clean 12.7-as pulse is generated by inverse Fourier transforming of the filtered spectrum in Fig. 5(b).

#220890 - $15.00 USD Received 12 Aug 2014; revised 23 Sep 2014; accepted 8 Oct 2014; published 16 Oct 2014

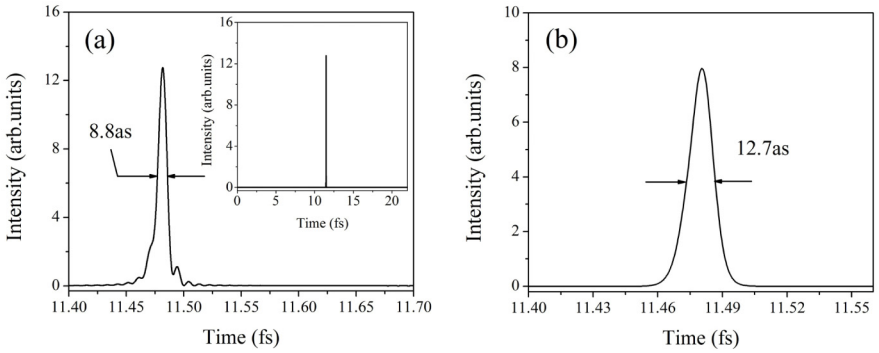

Fig. 5. (a) Attosecond pulse generation by superposing the harmonics from 1200th to 1500th order. Inset is attosecond pulse emission in the whole time range. (b) Attosecond pulse generation by using Gaussian band-pass function. The filter window (the FWHM of a Gaussian function) is set from 1200th to 1500th order which is identical to the frequency range in (a). The laser parameters used are the same as those in Fig. 3.

4. Conclusion

In summary, we study the harmonic emission of He atom in a spatially inhomogeneous two-color laser field, and propose an efficient scheme to produce ultrabroad supercontinuum in HHG. Our 3D quantum calculations demonstrate that this ultrabroad supercontinuum is generated by temporally controlling electronic recombination via adjusting the phase of the controlling laser. An isolated sub-10-attosecond pulse which is much shorter than the atomic unit can be produced with superposition of the supercontinuum harmonics. Note that the conversion efficiency of HHG is still a problem in strong laser fields with a proper non-homogeneity although the supercontinuum can be extended up to 1.5 keV, however, we expect that inhomogeneous two-color laser field will attract more attention into practical production of shorter attosecond pulse in future.

Acknowledgments

This work was supported by NSF of China Grant No. 21373113 and 60908006. C. Yu gratefully acknowledges the support of Scientific Research Innovation Projects of Jiangsu Province for University Graduate Students with Grant No. KYLX_0322. Y.-H. Wang gratefully acknowledges the support of Scientific Research Innovation Projects of Jiangsu Province for University Graduate Students with Grant No. CXZZ13_0201.

#220890 - $15.00 USD Received 12 Aug 2014; revised 23 Sep 2014; accepted 8 Oct 2014; published 16 Oct 2014